JOURNAL OF COMPUTATIONAL PHYSICS 95, 477–496 (1991)

Difference Formulas for the Surface Laplacian on a Triangulated Surface

GEERTJAN HUISKAMP

Laboratory of Medical Physics and Biophysics, University of Nijmegen, The Netherlands

Received March 13, 1989; revised June 14, 1990

Different approximating expressions for the surface Laplacian operator on a triangulated surface are derived. They are evaluated on a triangulated spherical surface for which the analytical expression of the surface Laplacian is known. It is shown that in order to obtain accurate results, due care has to be taken of irregularities present in the triangulation grid. If this is done, the approximation will equal the performance of an expression based on least squares which can be derived. Next the different approximations obtained are used as a regularization operator in the solution of an ill-posed inverse problem in electrical volume conduction. It is shown that in this application a crude approximation to the surface Laplacian suffices. © 1991 Academic Press, Inc.

INTRODUCTION

The Laplacian operator Δ is encountered in many fields of physics and applied mathematics. It turns up, e.g., in electrical volume conduction problems in physics and as a smoothing operator in many mathematical applications [1].

In this paper we will focus on the *surface* Laplacian, i.e., the restriction of the operator to two-dimensional flat space or to a (curved) surface in three dimensions. Among many other applications, the surface Laplacian operator can be used for interpolation and extrapolation purposes [2, 3], and for some smoothing operations, e.g., in picture processing [4]. It can also be used as a regularization operator in the solution of so-called *ill-posed* problems [5]. In this paper *Laplacian* should be interpreted as *surface Laplacian.*

In most of the practical applications, where analytical solutions of the problems involving the Laplacian operator cannot be obtained, one has to resort to approximating numerical expressions. This paper will describe some approximating expressions for the Laplacian operator which can be used on a triangulated 3D surface.

By way of introduction we will start by describing the well-known approximating expression for the Laplacian on a plane regular square grid. This expression leads to its generalization to a general plane regular grid. From this generalization, different expressions for the Laplacian will be derived on a general, triangulated

0021-9991/91 $3.00

flat surface. Assuming a sufficiently dense triangulation grid the same expressions can be used on a 3D *curved* surface. A strictly numerical method applicable to a curved 3D triangulated surface will also be presented.

The performance of these approximating expressions will be evaluated on a triangulated spherical surface on which some function, chosen more or less arbitrarily, is defined. In this situation, an analytical expression of the surface Laplacian can be derived which is used to validate the approximations. Next, the different approximations are tested in one practical application, i.e., as a regularization operator.

THEORY

The Plane Regular Square Grid

For a planar, regular, square grid a simple difference formula for the Laplacian operator Δ can be derived. Consider (Fig. 1) p_0 in such a grid, situated at the origin, with = neighbours $p_1, ..., p_4$ at a distance r. We will denote f_0 as the value of f at p_0 and f_i as the value at point p_i. A Taylor expansion in the x coordinate yields

$$f(r, 0) \simeq f(0, 0) + r \left.\frac{\partial f}{\partial x}\right|_{p_0} + \frac{1}{2} r^2 \left.\frac{\partial^2 f}{\partial x^2}\right|_{p_0}$$

or

$$f_1 \simeq f_0 + r \left.\frac{\partial f}{\partial x}\right|_{p_0} + \frac{1}{2} r^2 \left.\frac{\partial^2 f}{\partial x^2}\right|_{p_0}.$$

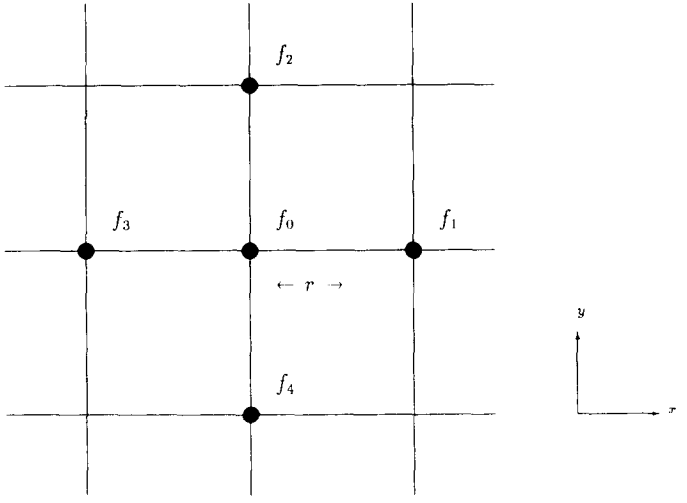

FIG. 1. A regular plane square grid.

For the y coordinate one has

$$f_2 \simeq f_0 + r \left.\frac{\partial f}{\partial y}\right|_{p_0} + \frac{1}{2} r^2 \left.\frac{\partial^2 f}{\partial y^2}\right|_{p_0}.$$

A similar expression can be found for f_3 and f_4. Addition of these four expressions yields

$$\begin{aligned} f_1 + f_2 + f_3 + f_4 &\simeq 4f_0 + r^2 \left.\left(\frac{\partial^2 f}{\partial x^2} + \frac{\partial^2 f}{\partial y^2}\right)\right|_{p_0} \\ &= 4f_0 + r^2 \, \Delta f|_{p_0}; \end{aligned}$$

hence, writing Δf_0 for $\Delta f|_{p_0}$,

$$\Delta f_0 \simeq \frac{1}{r^2}\left(\sum_{i=1}^{4} f_i - 4f_0\right),$$

i.e.,

$$\Delta f_0 \simeq \frac{4}{r^2}(\bar{f} - f_0), \tag{1}$$

in which $\bar{f}$ is the average of $f_1, \ldots, f_4$. This is the well-known first-order estimate of the Laplacian Δ on a regular square grid at p_0 [6].

Other Regular Plane Grids

Expression (1) can be generalized by taking the integral along a circle of radius r around p_0 of the truncated Taylor expansion. Defining $x = r\cos(\theta)$ and $y = r\sin(\theta)$ we have

$$\begin{aligned} \int_0^{2\pi} (f(r,\theta) - f_0)\, d\theta \simeq{}& r \int_0^{2\pi} \cos(\theta)\, d\theta \left.\frac{\partial f}{\partial x}\right|_{p_0} + r \int_0^{2\pi} \sin(\theta)\, d\theta \left.\frac{\partial f}{\partial y}\right|_{p_0} \\ &+ r^2 \int_0^{2\pi} \cos(\theta)\sin(\theta)\, d\theta \left.\frac{\partial^2 f}{\partial x\, \partial y}\right|_{p_0} \\ &+ \frac{1}{2} r^2 \int_0^{2\pi} \cos^2(\theta)\, d\theta \left.\frac{\partial^2 f}{\partial x^2}\right|_{p_0} + \frac{1}{2} r^2 \int_0^{2\pi} \sin^2(\theta)\, d\theta \left.\frac{\partial^2 f}{\partial y^2}\right|_{p_0}. \end{aligned}$$

Since the first three integrals on the right-hand side vanish and the remaining two give π, we have

$$\Delta f_0 = \left(\frac{\partial^2 f}{\partial x^2} + \frac{\partial^2 f}{\partial y^2}\right)\Big|_{p_0}$$
$$\simeq \frac{4}{r^2}\frac{1}{2\pi}\int_0^{2\pi} (f(r,\theta) - f_0)\, d\theta$$
$$= \frac{4}{r^2}(\overline{f - f_0}). \tag{2}$$

This generalization can be applied directly to plane regular grids (the regular hexagonal grid and the grid consisting of equilateral triangles). In general, for a single central point p_0 in a plane surrounded by N neighbours at equal angles and at distance r we can write down the expression

$$\Delta f_0 \simeq \frac{4}{r^2}\frac{1}{N}\sum_{i=1}^{N} (f_i - f_0)$$
$$= \sum_{i=1}^{N} w_i^{(0)}(f_i - f_0), \tag{3}$$

with weights

$$w_i^{(0)} = \frac{4}{r^2}\cdot\frac{1}{N}.$$

The Irregular Triangular Grid

The evaluation of expression (2) for an irregular triangulation of the plane is not straightforward. In general, the grid points will not be distributed regularly with equal distances between neighbouring points and equal angles between neighbours (as is the case with the regular grids mentioned). This breaking of symmetry has to be accounted for.

Regular Angles, Irregular Distances

When the N neighbouring points p_i are not regularly distributed around p_0, r in Eq. (3) could be replaced by $\bar{r}$, the mean distance to p_0. The approximation thus obtained, however, will in general be inaccurate, due to the breaking of symmetry.

However, when only the distances from neighbours p_i to p_0 differ and all angles are equal, symmetry can easily be restored by applying linear interpolation along the lines connecting p_0 to its neighbours. By replacing each neighbour p_i at distance r_i by a virtual neighbour $\tilde{p}_i$ at distance $\bar{r}$ along the same direction and assigning a value $\tilde{f}_i = f_0 + (\bar{r}/r_i)(f_i - f_0)$ to that point approximation (3) becomes

$$\begin{aligned}\Delta f_0 &\simeq \frac{4}{\bar{r}^2}\frac{1}{N}\sum_{i=1}^{N}(\bar{f}_i - f_0)\\ &= \frac{4}{\bar{r}}\frac{1}{N}\sum_{i=1}^{N}\frac{f_i - f_0}{r_i}\\ &= \sum_{i=1}^{N} w_i^{(1)}(f_i - f_0),\end{aligned} \tag{4}$$

with

$$w_i^{(1)} = \frac{4}{r}\cdot\frac{1}{N}\cdot\frac{1}{r_i}.$$

Irregular Angles, Irregular Distances

The approximation (4), when used in the situation where the neighbouring points are not distributed at regular angles around p_0, does not compensate for this breaking of symmetry. Therefore we return to Eq. (2) in which the mean value of f along a circle is involved.

Consider the situation as depicted in Fig. 2, representing a general situation for a triangular planar grid. We assume a linear interpolation scheme in order to obtain a value for f at $\mathbf{r}'$, with $\mathbf{r}'$ in the triangle with sides $\mathbf{r}_i$ and $\mathbf{r}_{i+1}$:

$$\mathbf{r}' = \lambda\mathbf{r}_i + \mu\mathbf{r}_{i+1}, \qquad f(\mathbf{r}') = f_0 + \lambda(f_i - f_0) + \mu(f_{i+1} - f_0),$$

with $\lambda, \mu \geq 0$. (The additional inequality $\lambda + \mu \leq 1$ is required if $\mathbf{r}'$ is *in* the triangle, but we allow $\mathbf{r}'$ to cross the edge $(\mathbf{r}_{i+1} - \mathbf{r}_i)$). If we take $\mathbf{r}'$ on a circle with radius r', to be specified later, we can express λ and μ in terms of r_i, r_{i+1}, r' and the angles α and ϕ_i,

$$\lambda = \frac{r'}{r_i}\frac{\sin(\phi_i - \alpha)}{\sin(\phi_i)}, \qquad \mu = \frac{r'}{r_{i+1}}\frac{\sin(\alpha)}{\sin(\phi_i)},$$

and, thus,

$$f(r', \alpha) - f_0 = \frac{r'}{r_i}\frac{\sin(\phi_i - \alpha)}{\sin(\phi_i)}(f_i - f_0) + \frac{r'}{r_{i+1}}\frac{\sin(\alpha)}{\sin(\phi_i)}(f_{i+1} - f_0).$$

We can now perform the integration of Eq. (2),

$$\begin{aligned}&\int_0^{2\pi}(f(r', \theta) - f_0)\,d\theta\\ &\quad= \sum_{i=1}^{N}\int_0^{\phi_i}\left(\frac{r'}{r_i}\frac{\sin(\phi_i - \alpha)}{\sin(\phi_i)}(f_i - f_0) + \frac{r'}{r_{i+1}}\frac{\sin(\alpha)}{\sin(\phi_i)}(f_{i+1} - f_0)\right)d\alpha\\ &= \sum_{i=1}^{N}\left[\frac{r'}{r_i}\cdot\frac{1 - \cos(\phi_i)}{\sin(\phi_i)}(f_i - f_0) + \frac{r'}{r_{i+1}}\cdot\frac{1 - \cos(\phi_i)}{\sin(\phi_i)}(f_{i+1} - f_0)\right].\end{aligned}$$

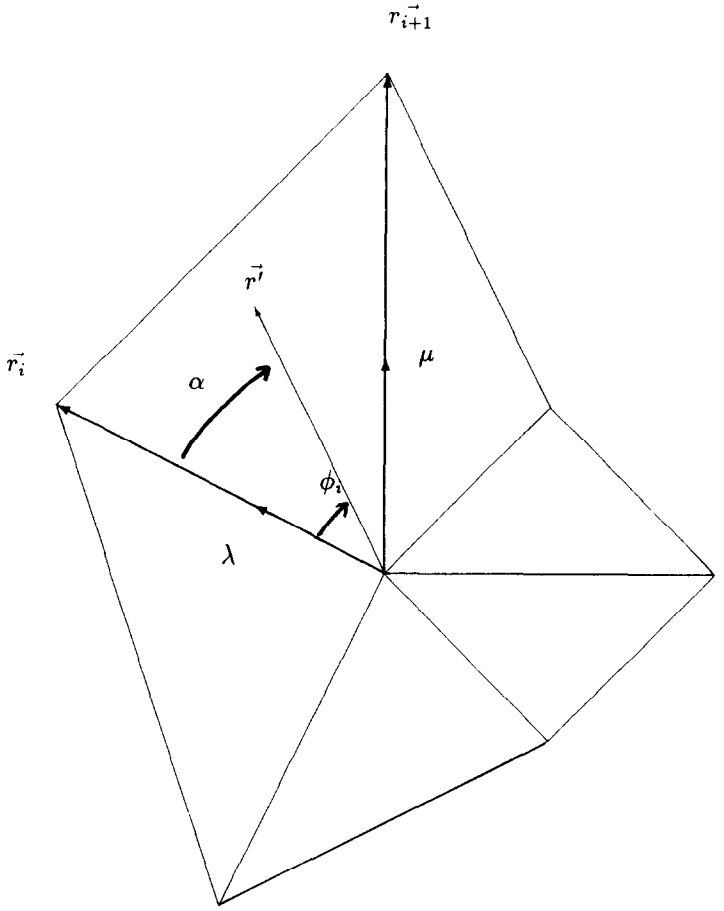

FIG. 2. An irregular plane triangular grid.

Reordering terms and defining ϕ_i^+ as the angle from $\mathbf{r}_i$ to $\mathbf{r}_{i+1}$ and ϕ_i^- as the angle from $\mathbf{r}_{i-1}$ to $\mathbf{r}_i$, $\mathbf{r}_0$ being $\mathbf{r}_N$ and $\mathbf{r}_{N+1}$ being $\mathbf{r}_1$, we have

$$\int_0^{2\pi} (f(r', \theta) - f_0)\, d\theta = \sum_{i=1}^{N} \frac{r'}{r_i} \left(\frac{1-\cos(\phi_i^-)}{\sin(\phi_i^-)} + \frac{1-\cos(\phi_i^+)}{\sin(\phi_i^+)} \right) (f_i - f_0).$$

This leads to the approximation (cf. Eq. (2))

$$\Delta f_0 \simeq \frac{4}{r'} \frac{1}{2\pi} \sum_{i=1}^{N} \left(\frac{1-\cos(\phi_i^-)}{\sin(\phi_i^-)} + \frac{1-\cos(\phi_i^+)}{\sin(\phi_i^+)} \right) \frac{f_i - f_0}{r_i}.$$

We now choose r' to be such that in the case of equal angles ϕ_i the approximation reduces to expression (4):

$$r' = \bar{r}\frac{\Phi_{\text{tot}}}{2\pi}, \qquad \text{with} \quad \Phi_{\text{tot}} = \sum_{i=1}^{N}\left(\frac{1-\cos(\phi_i^-)}{\sin(\phi_i^-)} + \frac{1-\cos(\phi_i^+)}{\sin(\phi_i^+)}\right).$$

This finally leads to the approximation

$$\Delta f_0 \simeq \sum_{i=1}^{N} w_i^{(2)}(f_i - f_0), \tag{5}$$

with

$$w_i^{(2)} = \frac{4}{\bar{r}} \cdot \frac{1}{\Phi_{\text{tot}}} \cdot \frac{1}{r_i}\left(\frac{1-\cos(\phi_i^-)}{\sin(\phi_i^-)} + \frac{1-\cos(\phi_i^+)}{\sin(\phi_i^+)}\right).$$

The Formulation as a Least Squares Problem

Consider the central point p_0, situated at the origin for convenience, with function value f_0, which is surrounded by N neighbours $p_i = (x_i, y_i)$ with value f_i. For each p_i we again look at the Taylor expansion of f around p_0:

$$f_i \simeq f_0 + x_i\left.\frac{\partial f}{\partial x}\right|_{p_0} + y_i\left.\frac{\partial f}{\partial y}\right|_{p_0} + x_i y_i\left.\frac{\partial^2 f}{\partial y\,\partial x}\right|_{p_0} + \frac{1}{2}x_i^2\left.\frac{\partial^2 f}{\partial x^2}\right|_{p_0} + \frac{1}{2}y_i^2\left.\frac{\partial^2 f}{\partial y^2}\right|_{p_0}.$$

By using the notation $\partial_x = \partial/\partial x$, $\partial_x^2 = \partial^2/\partial x^2$, ..., etc. and $\delta f_i = f_i - f_0$, this expansion can be written as a matrix equation:

$$\begin{pmatrix} \frac{1}{2}x_1^2 & \frac{1}{2}y_1^2 & x_1 y_1 & x_1 & y_1 \\ \frac{1}{2}x_2^2 & \frac{1}{2}y_2^2 & x_2 y_2 & x_2 & y_2 \\ \vdots & & & & \vdots \\ \frac{1}{2}x_N^2 & \frac{1}{2}y_N^2 & x_N y_N & x_N & y_N \end{pmatrix} \begin{pmatrix} \partial_x^2 f \\ \partial_y^2 f \\ \partial_{xy}^2 f \\ \partial_x f \\ \partial_y f \end{pmatrix} \simeq \begin{pmatrix} f_1 - f_0 \\ f_2 - f_0 \\ \vdots \\ f_N - f_0 \end{pmatrix},$$

or

$$D\mathbf{d} \simeq \delta\mathbf{f}.$$

This matrix equation can be solved uniquely in a least squares sense, provided that the number of neighbours N is greater than or equal to five and that the matrix columns are independent. Even in the case of linear dependency a least squares solution having minimal norm may be computed as

$$\mathbf{d} \simeq D^{\dagger}\delta\mathbf{f},$$

with $D^{\dagger}$ a pseudo inverse obtained through the *singular value decomposition* of the matrix D [7]. In this approach N may even be less than five.

From this expression an approximation to the Laplacian Δ may be formulated as

$$\Delta f_0 = \left(\frac{\partial^2 f}{\partial x^2} + \frac{\partial^2 f}{\partial y^2}\right)\Big|_{p_0} \simeq \sum_{i=1}^{N} (D_{1i}^{\dagger} + D_{2i}^{\dagger})\, \delta f_i$$
$$= \sum_{i=1}^{N} w_i^{(3)}(f_i - f_0), \tag{6}$$

with

$$w_i^{(3)} = D_{1i}^{\dagger} + D_{2i}^{\dagger}.$$

Here $D_{1i}^{\dagger}$ and $D_{2i}^{\dagger}$ refer to the ith components of the first and second rows of the pseudo inverse $D^{\dagger}$. This approach with planar cartesian coordinates (x, y) can be adapted to one resulting in an expression in the local surface coordinates (ξ, η) on a curved surface in three dimensions.

Better approximations can be obtained by assigning different weights (e.g., the inverse distance to the central point) to the different rows of the matrix equation given above.

Test Procedures

Evaluation on a Triangulated Spherical Surface

In order to test the different approximations of Eqs. (3), (4), (5), and (6), to which we will refer as $\Delta^{(0)}$, $\Delta^{(1)}$, $\Delta^{(2)}$, and $\Delta^{(3)}$, respectively, triangulations were made of the surface of a sphere. The well-known expression for the surface Laplacian operator on a sphere, in spherical coordinates r, θ, and ϕ, is

$$\Delta = \frac{1}{r^2}\frac{\partial^2}{\partial\theta^2} + \frac{\cos(\theta)}{r^2 \sin(\theta)}\frac{\partial}{\partial\theta} + \frac{1}{r^2 \sin^2(\theta)}\frac{\partial^2}{\partial\phi^2}.$$

As an analytical test function, a function of the form

$$f(\theta, \phi) = \sum_{i=1}^{M} F(\mathbf{R}_i \cdot \hat{n}(\theta, \phi))$$

was used. Here $\hat{n}(\theta, \phi)$ is a unit surface normal, $\mathbf{R}_i$ is a vector of arbitrary length and direction, and F is a real-valued function that is at least two times differentiable. $M = 12$ vectors $\mathbf{R}_i$ with random direction and random length between 0 and 1 were chosen, F was taken to be $F(t) = \sin(\pi t)$.

Two distinct triangulations of the sphere were made: one in which the distribution of points was as regular as possible and one which was highly irregular. Of this

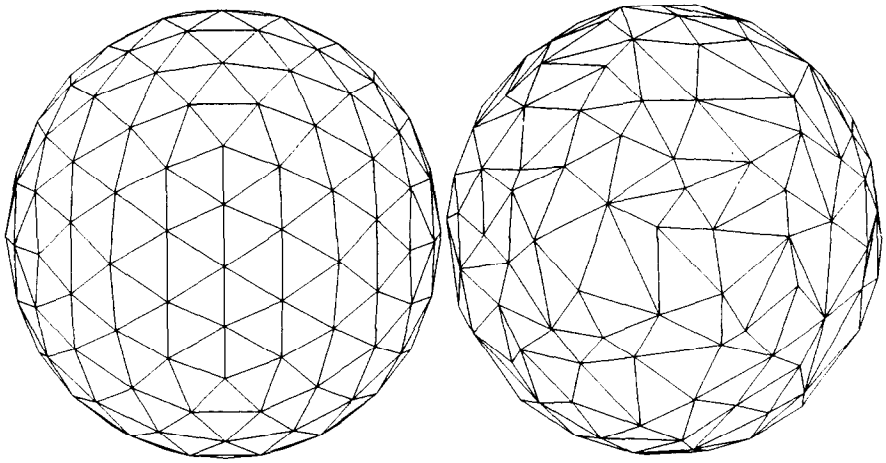

FIG. 3. Frontal view of the 162-point regular triangulation of the sphere (left) and of the 162-point irregular triangulation (right).

first regular triangulation three variants, consisting of 42, 162, and 642 points, respectively, were tested. For the irregular triangulation a version consisting of 162 points and one of 642 points were chosen. Figure 3 shows a frontal view of the regular (left) and the irregular (right) triangulations of the sphere, both consisting of 162 points.

The chosen function f and its analytical Laplacian (left- and right-hand side, respectively) are depicted, from the same perspective, in Fig. 4 as isofunction lines on the regular sphere, obtained through linear interpolation. Maximum and minimum value for f are 6.07 and -6.07 and a stepsize of 0.5 was used. Negative values for f appear dashed. Maximum and minimum value for the analytical Laplacian of f on the sphere are 63.3 and -63.5 and a stepsize of 5.0 was chosen.

For each of the triangulations, the approximations $\Delta^{(0)}, \ldots, \Delta^{(3)}$ to the surface Laplacian of the function f at each vertex were calculated and compared to the values for the analytical Laplacian. In approximation $\Delta^{(3)}$ local coordinates for the curved surface were used. As indicated earlier, expressions $\Delta^{(0)}$, $\Delta^{(1)}$, and $\Delta^{(2)}$ were applied without modifications, thus neglecting the curvature of the sphere.

As a means of comparison, a relative rms and an absolute maximal difference measure on the triangulated surface X were defined as

$$\text{RELDIFF}^i = \left[\frac{\int_X (\Delta f(x) - \Delta^{(i)} f(x))^2 \, dx}{\int_X (\Delta f(x))^2 \, dx} \right]^{1/2}$$

and

$$\text{MAXDIFF}^i = \max_{x \in X} |\Delta f(x) - \Delta^{(i)} f(x)|.$$

Here Δ refers to the analytical Laplacian and $\Delta^{(i)}$ to one of the approximations $\Delta^{(0)}, \ldots, \Delta^{(3)}$. The surface integrals involved were calculated by using an approximating surface area for each vertex.

Evaluation as a Regularization Operator

Let a triangulated 3D surface be described by N labelled point p_i and let each point p_i be surrounded by M_i neighbours labelled nb_k^i (i.e., $nb_k^i = j$ if p_j is the kth neighbour of p_i). With the expression for an approximation of the Laplacian operator at point p_i of the form

$$\Delta f(p_i) \simeq \sum_{k=1}^{M_i} w_{ik}(f(p_{nb_k^i}) - f(p_i)),$$

a matrix L can be defined which when multiplied with the vector $\mathbf{f}$, $f_i = f(p_i)$, gives the vector $\boldsymbol{\Delta}$ of values of the Laplacian at each point p_i:

$$\begin{aligned} L_{ij} &= w_{ik} && \text{if } i \neq j \text{ and } p_j \text{ is the } k\text{th neighbour of } p_i, \\ &= 0 && \text{if } i \neq j \text{ and } p_j \text{ is not a neighbour of } p_i, \\ &= -\sum_{k=1}^{M_i} w_{ik} && \text{if } i = j, \end{aligned}$$

or

$$L_{ij} = \sum_{k=1}^{M_i} \delta_{jnb_k^i} w_{ik} - \delta_{ij} \sum_{k=1}^{M_i} w_{ik}. \tag{7}$$

This matrix expression for Δ was used as a regularization operator in a solution method for the inverse problem of electrocardiography of the form [8]:

$$\text{Minimize} \qquad E(\tau) = |Af(\tau) - \mathbf{v}|^2 + \lambda |L\tau|^2. \tag{8}$$

The vector τ here describes the moment of electrical activation, expressed in milliseconds, of points on the (triangulated) surface of the heart; $\mathbf{v}$ is a vector containing the values of potentials measured on the torso surface; and the matrix A describes the volume conductor properties of the torso; $|\cdot|$ denotes the Euclidian norm. The inverse problem of electrocardiography belongs to the class of *ill-conditioned* problems, implying that small variations in measurement data (A and $\mathbf{v}$) may cause large variations in the solution τ. The purpose of the Laplacian operator in this minimization problem is to keep solutions τ bounded and smooth, in keeping with the physiological knowledge on the properties of the electrical activation process of the heart.

With the accuracy of the triangulation of the heart surface having been chosen in accordance with the physiologically expected variation of τ over that surface, the

different matrix expressions $L^{(0)}$, $L^{(1)}$, $L^{(2)}$, and $L^{(3)}$ relating to the approximations $\Delta^{(0)}$, $\Delta^{(1)}$, $\Delta^{(2)}$, and $\Delta^{(3)}$ were used as regularization operators. Their differences in performance were evaluated by comparing the difference between solutions $\tau^{(i)}$ on the basis of measures similar to RELDIFF and MAXDIFF, as defined in the previous section:

$$\text{RELDIFF}^{ij} = \left[\frac{\int_X (\tau^{(i)}(x) - \tau^{(j)}(x))^2 \, dx}{\int_X (\tau^{(i)})^2 \, dx} \right]^{1/2};$$

$$\text{MAXDIFF}^{ij} = \max_{x \in X} |\tau^{(i)}(x) - \tau^{(j)}(x)|.$$

Additionally, the approximations $\Delta^{(0)}, \ldots, \Delta^{(3)}$ to the surface Laplacian of the solution $\tau^{(3)}$ on the triangulated heart surface were compared mutually, using a RELDIFF^{ij} measure.

RESULTS

The Triangulated Sphere

Results for the different approximations $\Delta^{(0)}$ (upper left), $\Delta^{(1)}$ (upper right), $\Delta^{(2)}$ (lower right, and $\Delta^{(3)}$ (lower left) are shown in Fig. 5 for the regular sphere (162 points) and in Fig. 6 for the irregular sphere (162 points). The viewpoint and the stepsize are as chosen in Fig. 4 for the analytical Laplacian. Figure 7 shows the the refined regular sphere, consisting of 642 points, and the approximation $\Delta^{(0)}$ on it. The difference measures for both the original and the refined triangulations are summarized in Table I.

TABLE I

RELDIFF and MAXDIFF Values for Laplacian Approximations on Regularly and Irregularly Discretized Spheres

	$\Delta^{(0)}$		$\Delta^{(1)}$		$\Delta^{(2)}$		$\Delta^{(3)}$	
Regular	REL	0.302	REL	0.305	REL	0.304	REL	0.303
42 pnts.	MAX	20.1	MAX	20.0	MAX	20.1	MAX	19.9
Regular	REL	0.163	REL	0.133	REL	0.095	REL	0.094
162 pnts.	MAX	13.5	MAX	10.1	MAX	6.1	MAX	6.0
Regular	REL	0.292	REL	0.197	REL	0.043	REL	0.027
642 pnts.	MAX	36.2	MAX	27.9	MAX	4.1	MAX	2.1
Irregular	REL	0.568	REL	0.399	REL	0.201	REL	0.155
162 pnts.	MAX	59.0	MAX	30.7	MAX	16.6	MAX	11.2
Irregular	REL	1.050	REL	0.728	REL	0.170	REL	0.059
642 pnts.	MAX	178.9	MAX	150.6	MAX	22.7	MAX	9.5

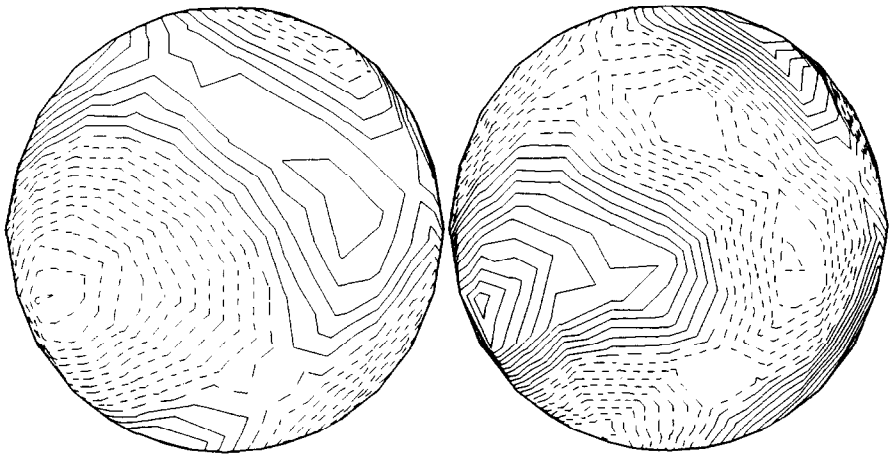

FIG. 4. Isofunction lines of the chosen function f (left) and its analytical Laplacian Δf (right), plotted on the regulary triangulated surface of Fig. 3. Linear interpolation is used. The stepsize is 0.5 for f and 5.0 for Δf (arbitrary units). Negative values appear dashed.

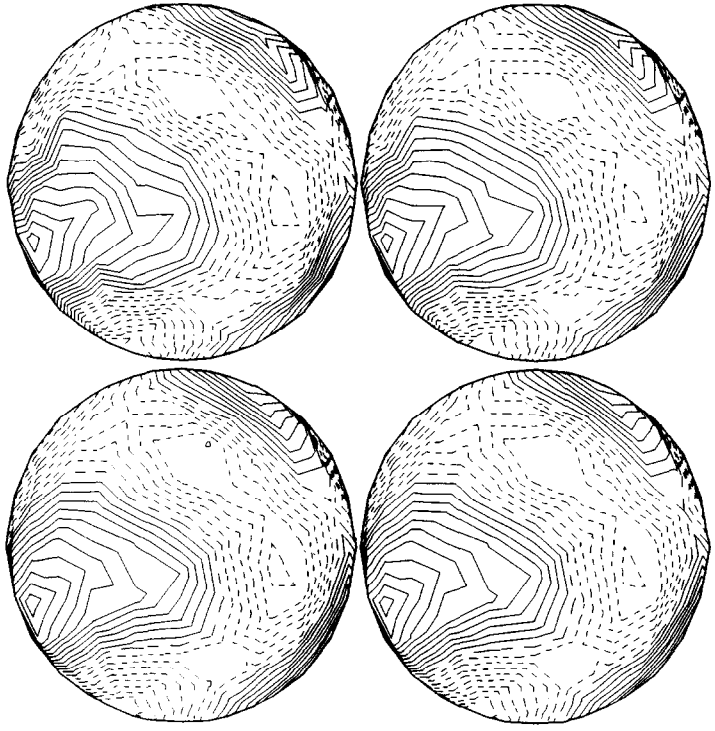

FIG. 5. Isofunction lines of approximation $\Delta^{(0)}f$ (upper left), $\Delta^{(1)}f$ (upper right), $\Delta^{(2)}f$ (lower right), and $\Delta^{(3)}f$ (lower left) on the 162-point *regular* sphere. View and stepsize as in right-hand side of Fig. 4.

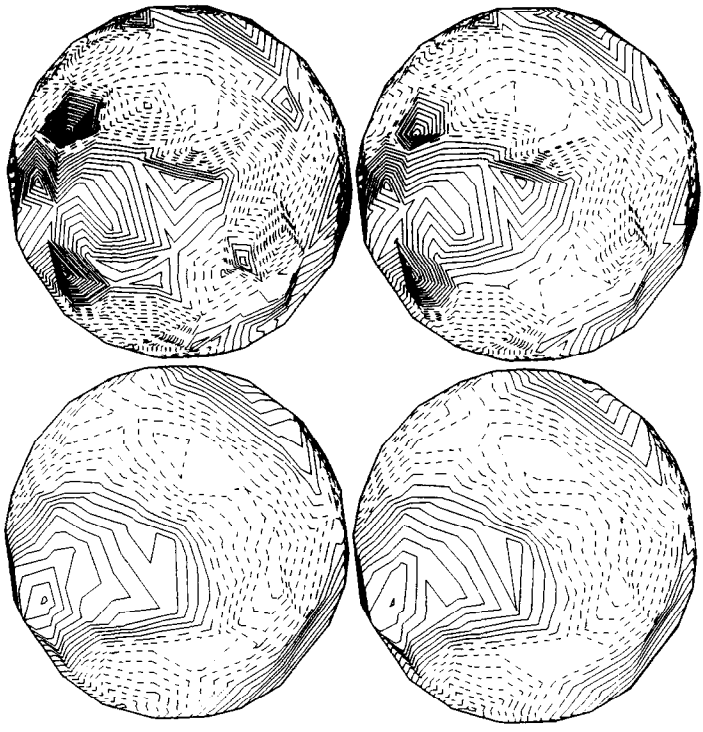

FIG. 6. Isofunction lines of approximations $\Delta^{(0)}f$ (upper left), $\Delta^{(1)}f$ (upper right), $\Delta^{(2)}f$ (lower right), and $\Delta^{(3)}f$ (lower left) on the 162-point *irregular* sphere. View and stepsize as in Fig. 4.

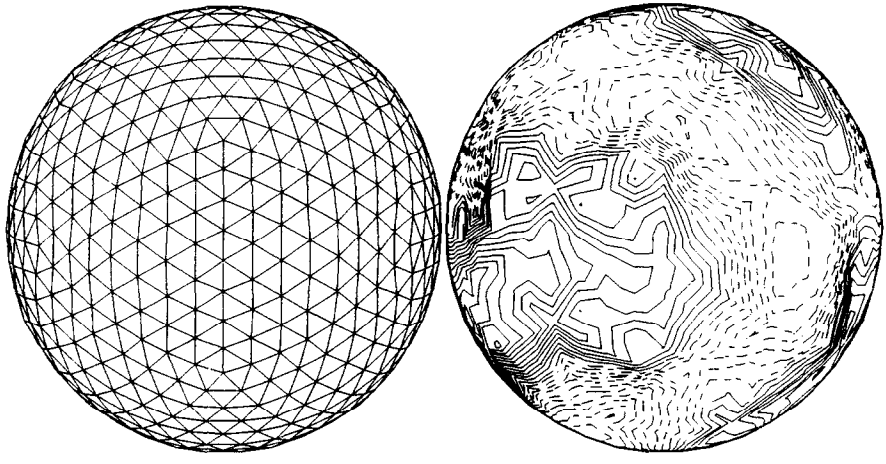

FIG. 7. 642-point, refined regular triangulation of the sphere (left) and isofunction lines of approximation $\Delta^{(0)}f$ on it (right). View and stepsize as in Fig. 4.

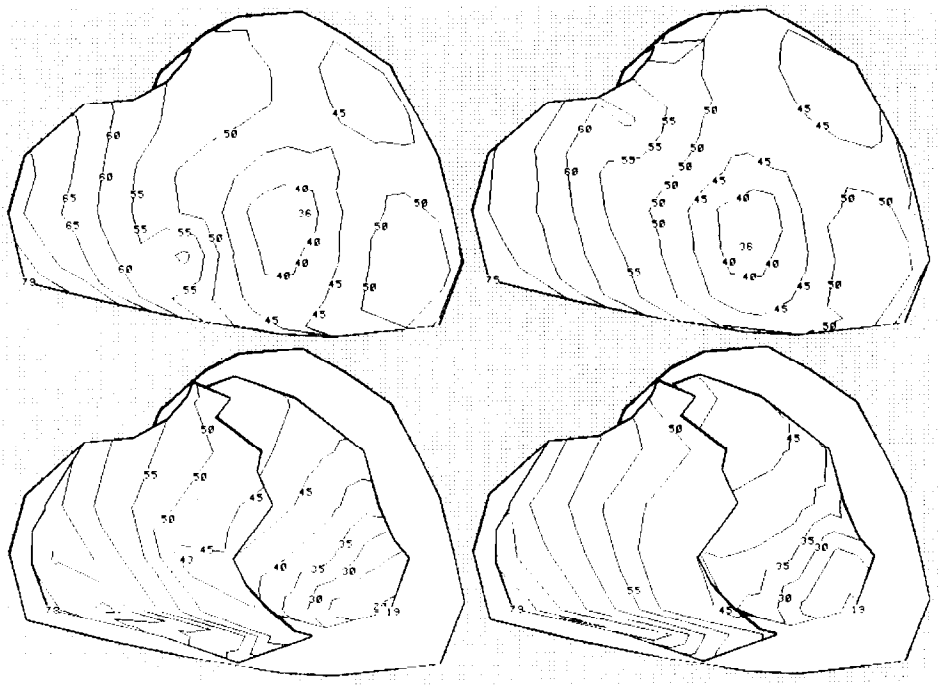

FIG. 8. Isochrones of activation-functions $\tau^{(3)}$ (left) and $\tau^{(0)}$ (right) on the triangulated surface of the human heart. The stepsize is 5 ms. Upper part shows a frontal view of the outside of the heart (epicardium), lower part shows the inside in the same view (endocardium).

The Regularization Operator

In Table II all relative and maximum differences between the solutions $\tau^{(i)}$, $i = 0$, 3, are given. Figure 8 shows the solutions $\tau^{(3)}$ and $\tau^{(0)}$ obtained when using the approximations $\Delta^{(3)}$ and $\Delta^{(0)}$ as regularization operators. RELDIFF and MAXDIFF values between approximations $\Delta^{(i)}$, $i = 0$, 3, to the surface Laplacian of the function $\tau^{(3)}$ are given in Table III.

DISCUSSION

Comparison between the results obtained with the approximations $\Delta^{(0)}, \ldots, \Delta^{(3)}$ for the regular, unrefined sphere, as shown in Fig. 5, and the analytical Laplacian of Fig. 4 show only small differences on the basis of visual inspection. Evaluation of the measures (Table I), however, shows that the performance of the approximations $\Delta^{(0)}$ and $\Delta^{(1)}$ is worse than that of $\Delta^{(2)}$ and $\Delta^{(3)}$, in terms of both relative and absolute differences.

Although the differences are not dramatic, small variations in the angles of the

triangular tiles cause poorer performance in the approximations in which these irregularities are not considered.

This effect is, surprisingly, amplified when the refined triangulation of the sphere is used. Although an improvement of the approximation can be expected when more points are chosen on the sphere, the effect of disregarding irregular angles worsens the approximations $\Delta^{(0)}$ and $\Delta^{(1)}$, whereas by taking them into account the approximations $\Delta^{(2)}$ and $\Delta^{(3)}$ are improved (see Appendix).

The use of a manifestly irregular triangulation of the sphere results in very bad approximations $\Delta^{(0)}$ and $\Delta^{(1)}$, both with respect to the different values and on the basis of visual inspection (Fig. 6). Refinement of the triangulation again worsens matters for $\Delta^{(0)}$ and $\Delta^{(1)}$.

Approximation $\Delta^{(3)}$ performs best in all cases presented, and when compared to $\Delta^{(2)}$, the difference in performance is largest in the case of the irregular refined sphere. This improved performance cannot be explained by the fact that in $\Delta^{(3)}$ the curvature of the surface is taken into account, since a refinement of the triangulation implies a more flat neighbourhood for each point, thus decreasing the effect of disregarding the curvature. The explanation lies in the fact that in $\Delta^{(3)}$ a least squares approximation to the Taylor expansion is used, thus explicitly minimizing the difference between the analytical and the approximated Laplacian. Smaller differences in performance between $\Delta^{(2)}$ and $\Delta^{(3)}$ for the spheres having fewer discretization points can be explained by the growing dominance of the error resulting from taking a sampling grid which is too sparse, given the function defined on the sphere.

Summarizing, it is shown that the irregularities in the triangulations must be incorporated into an approximating expression for the Laplacian operator. Only when the discretization is chosen such that "undersampling" occurs is the performance of all approximations roughly the same. It is also shown that approximation $\Delta^{(3)}$ performs best. However, when the number of discretization points is large enough to reflect the variation of the function chosen (cf. Fig. 4), approximation

TABLE II

RELDIFF^{ij} and MAXDIFF^{ij} Values for Pairs of Solutions $\tau^{(i)}$, $\tau^{(j)}$ Related to the Use of $\Delta^{(0)}, \ldots, \Delta^{(3)}$ as Regularization Operator

	$\tau^{(0)}$		$\tau^{(1)}$		$\tau^{(2)}$		$\tau^{(3)}$	
Reference	REL	—	REL	0.024	REL	0.045	REL	0.054
$\tau^{(0)}$	MAX	—	MAX	4.91	MAX	9.96	MAX	11.4
Reference	REL	0.025	REL	—	REL	0.035	REL	0.055
$\tau^{(1)}$	MAX	4.91	MAX	—	MAX	8.12	MAX	11.0
Reference	REL	0.045	REL	0.035	REL	—	REL	0.046
$\tau^{(2)}$	MAX	9.96	MAX	8.12	MAX	—	MAX	10.9
Reference	REL	0.054	REL	0.055	REL	0.046	REL	—
$\tau^{(3)}$	MAX	11.4	MAX	11.0	MAX	10.9	MAX	—

TABLE III

Mutual RELDIFF Values for Different Approximations $\Delta^{(i)}$, $\Delta^{(j)}$ to the Laplacian of the Function $\tau^{(3)}$ on the Heart Surface

	$\Delta^{(0)}$		$\Delta^{(1)}$		$\Delta^{(2)}$		$\Delta^{(3)}$	
$\Delta^{(0)}$	REL	—	REL	0.19	REL	0.46	REL	0.65
$\Delta^{(1)}$	REL	0.20	REL	—	REL	0.37	REL	0.63
$\Delta^{(2)}$	REL	0.45	REL	0.35	REL	—	REL	0.52
$\Delta^{(3)}$	REL	0.54	REL	0.50	REL	0.44	REL	—

$\Delta^{(2)}$ is still a good choice. It has the advantage of greater conceptual simplicity because it can be expressed directly in terms of the angles and distances between points and their neighbours, whereas $\Delta^{(3)}$ requires, for each point of the triangulation, the solution of a least squares system.

When applying each of the approximations $\Delta^{(0)}, \ldots, \Delta^{(3)}$ as a regularization operator in the ill-conditioned problem presented here, variations in the solutions appear to be within the limits imposed by the sensitivity of the problem to modelling and measurement noise [9].

Tables II and III show that in the regularization of ill-conditioned problems, such as the one presented here, a relatively crude approximation to the Laplacian operator will suffice. While the differences in the inverse solutions obtained are at most 5.5%, the differences between the approximations to the Laplacian are much bigger, indicating that at most only one of the approximations is not "crude."

In the scattered data fitting literature more elaborate schemes exist, which will give better approximations to the function to be interpolated and its partial (second-order) derivatives [10, 11]. Such methods may consider more points than the restricted number of neighbours implied by the triangulation used here; i.e., more global information of the function is used. We feel, however, that in the application given here, confined to the framework of the triangulation, the method presented provides a straightforward and fast algorithm for obtaining an approximation to the surface Laplacian on a triangulated surface.

APPENDIX

In this appendix the poorer performance of the crude approximations $\Delta^{(0)}$ and $\Delta^{(1)}$, which occurs when the triangular grid is refined, is discussed.

Suppose there exists an accurate approximation Δ for the Laplacian operator on a planar surface which can be expressed as (cf. Eq. (5))

$$\Delta f_0 = \frac{4}{\bar{r}} \sum_i^N q_i \frac{(f_i - f_0)}{r_i},$$

where the weights q_i depend only on the interior angles of the triangular tiles, and a second, less accurate, approximation with erroneous weights $(q_i + \varepsilon_i)$ (cf. Eq. (4))

$$\begin{aligned}\tilde{\Delta} f_0 &= \frac{4}{\bar{r}} \sum_i^N (q_i + \varepsilon_i) \frac{(f_i - f_0)}{r_i} \\ &= \Delta f_0 + \Xi f_0\end{aligned}$$

with

$$\Xi f_0 = \frac{4}{\bar{r}} \sum_i^N \varepsilon_i \frac{(f_i - f_0)}{r_i}.$$

For each i we can write the Taylor expansion of f about p_0 in the direction of $\mathbf{r}_i$ $(= p_i - p_0)$:

$$\begin{aligned}\Xi f_0 &= \frac{4}{\bar{r}} \sum_i^N \varepsilon_i \frac{1}{r_i} \left(r_i \frac{\partial f}{\partial \hat{r}_i}\bigg|_{p_0} + \frac{r_i^2}{2} \frac{\partial^2 f}{\partial \hat{r}_i^2}\bigg|_{p_0} + \cdots \right) \\ &= 4 \sum_i^N \varepsilon_i \left(\frac{1}{\bar{r}} \frac{\partial f}{\partial \hat{r}_i}\bigg|_{p_0} + \frac{r_i}{2\bar{r}} \frac{\partial^2 f}{\partial \hat{r}_i^2}\bigg|_{p_0} + \cdots \right).\end{aligned}$$

The Taylor expansion is truncated at the second-order derivative, since in the derivation of the approximating expression to the Laplacian, higher order terms were neglected in the first place. Therefore if $\bar{r}$ and r_i are chosen big with respect to the variations of f the error of the approximation will grow, regardless of (a)symmetry of the angles.

When, on the other hand, the truncation of the Taylor expansion is justified, a refinement of the triangular mesh (cf. Fig. 3 and Fig. 6) implies $\bar{r}$, $r_i \to 0$ while all other terms remain the same, which means that Ξ, i.e., the error in the approximation $\tilde{\Delta}$ due to erroneous weight factors w_i, will grow (provided that the norm of the gradient at p_0, relating to $\partial f / \partial \hat{r}_i |_{p_0}$, is greater than 0).

The effect is demonstrated in Table A and in Fig. A1 and A2. Here the approximation $\Delta^{(1)}$ on a (finite) regular hexagonal plane grid is treated. A slightly distorted version of this grid, where for each point the weight factors w_i differ only about 1% from the mean value $\frac{1}{6}$, is also available. For both of these (61 point-) grids, two successive refinements are made, consisting of 217 and 817 points, respectively. As a test function a function similar to the one used previously is chosen. Because in points on the rim the calculation of the approximation to the Laplacian cannot be performed, for these points values of Δ and $\Delta^{(1)}$ have been determined by iteratively averaging the values of neighbouring points.

Figure A1 shows the test function in a grey scale representation (left upper panel). The maximum value is depicted black, the minimum value white, with $f = 0$ at the middle grey level. The upper right panel shows the analytical Laplacian of f, again with maximum value black and zero at the middle grey level. The lower left

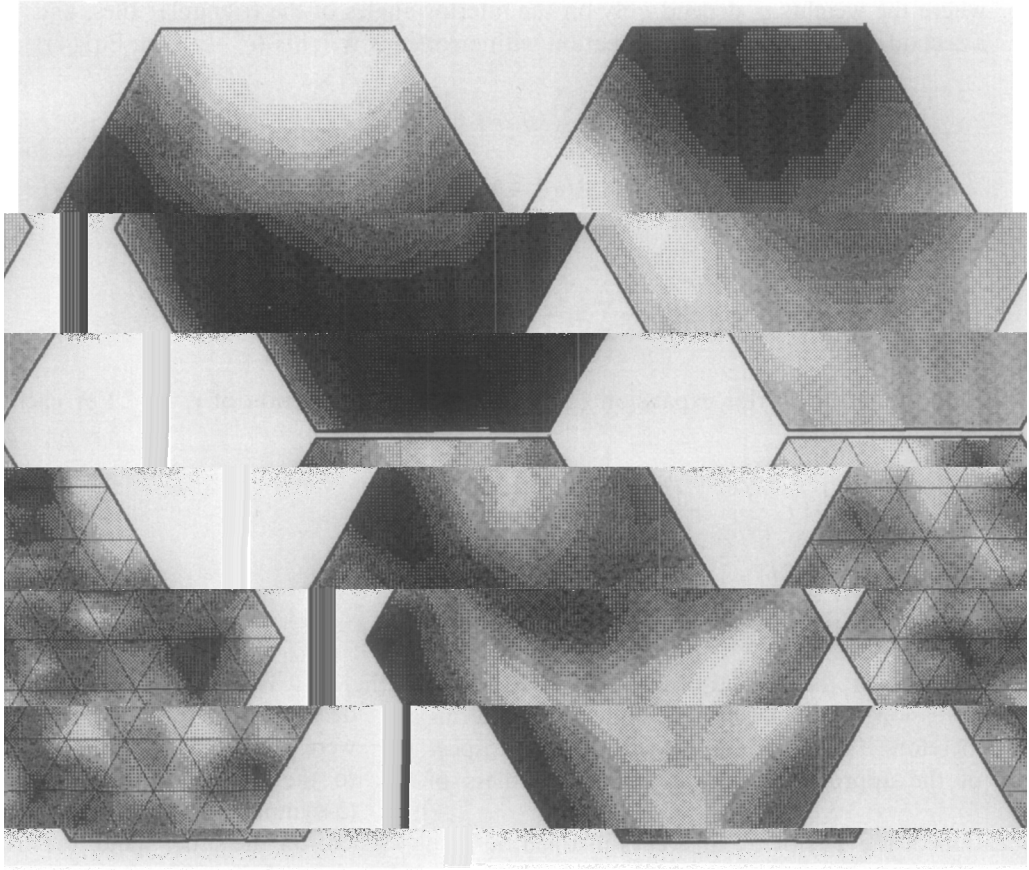

FIG. A1. (a) Grey scale representation of the chosen function f (upper left) on the hexagonal grid; black represents the maximum value, $f=0$ at the middle grey level. (b) Analytical Δf (upper right), maximum value black, zero at middle grey level. (c) $|\nabla f|$ (lower left), scaled between its maximum and minimum value. (d) Triangular grid and standard deviation of the angular weight factors for the distorted grid (lower right); grey scale for standard deviation goes from minimum to maximum value occurring.

panel shows the norm of the (analytical) gradient vector of f, scaled between its maximum and minimum value. Finally, the lower right panel shows the triangles composing the distorted grid and the standard deviation of the angular weight factors, scaled between the maximum and minimum values occurring. Notice that the deviation from the regular hexagonal grid is too small to be visible in the plot of the triangles.

The performance of approximation $\Delta^{(1)}$ on the various hexagonal grids is summarized in Table A. The left column shows the decrease of RELDIFF and MAXDIFF when the *regular* grid is refined, while the right column shows the

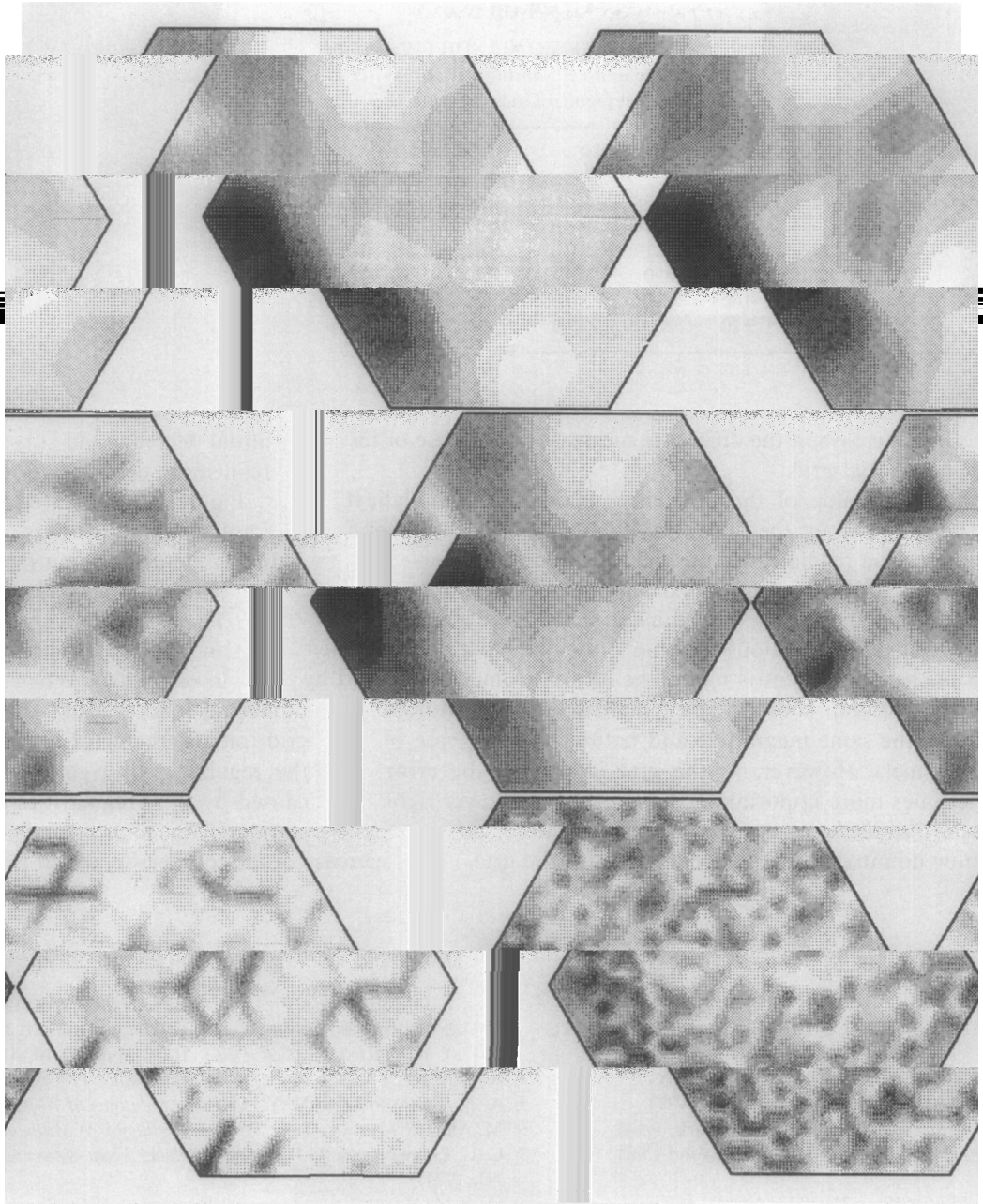

FIG. A2. $|\Delta^{(1)}f - \Delta f|$ for different hexagonal grids. Each plot is scaled to the maximum and minimum values occurring in it. Left column, from top to bottom: 61-, 217-, and 817-point regular hexagonal grid. Right column: 61-, 217-, and 817-point distorted grid.

TABLE A

RELDIFF and MAXDIFF Values for Approximation $\Delta^{(1)}$ on the Various Hexagonal Grids

Points	Regular		Distorted	
61	REL	0.068	REL	0.067
	MAX	17.3	MAX	16.3
217	REL	0.019	REL	0.027
	MAX	4.90	MAX	8.30
817	REL	0.008	REL	0.035
	MAX	2.20	MAX	17.3

initial decrease and subsequent increase of the difference measures in the case of the refinement of the *distorted* hexagonal grid.

Figure A2 shows the absolute value of the differences between the analytical Laplacian and the approximation $\Delta^{(1)}$ for the grids. The different panels correspond to Table A: the left column represents the regular grid, the right column the distorted one. Each plot is scaled to the maximum and minimum values occurring in it. The left column shows that for the regular hexagonal grid the error made in the 61- and 217-point cases is related to variations in f itself (compare $|\nabla f|$, Fig. A1, left lower panel). When a further refinement is made, the error becomes dominated by numerical inaccuracies. The right column shows that in the case of the distorted grid initially the error made is of the same magnitude and nature as in the case of the regular grid (right upper panel). However, as the grid is refined, the error caused by the irregularities becomes more important (compare Fig. A1, lower right panel), although the total error is still decreasing. A further refinement causes an increase of the total error, which is now dominated by the irregularities of the grid.

REFERENCES

1. D. L. PHILLIPS, *J. Assoc. Comput. Mach.* **9**, 4 (1962).
2. T. F. OOSTENDORP, A. VAN OOSTEROM, AND G. J. M. HUISKAMP, *J. Comput. Phys.* **80**, 331 (1989).
3. R. J. RENKA, *ACM Trans. Math. Software* **10**, 417 (1984).
4. A. ROSENFELD AND A. C. KAK, *Digital Picture Processing* (Academic Press, New York, 1976).
5. A. N. TIKHONOV AND V. Y. ARSENIN, *Solutions of Ill-posed Problems* (Wiley, New York, 1977).
6. M. ABRAMOWITZ AND I. A. STEGUN, *Handbook of Mathematical Functions* (Dover, New York, 1964).
7. C. L. LAWSON AND R. J. HANSON, *Solving Least Squares Problems* (Prentice-Hall, Englewood Cliffs, NJ, 1974).
8. G. J. M. HUISKAMP AND A. VAN OOSTEROM, *IEEE Trans. Biomed. Eng.* **35**, 1047 (1988).
9. G. J. M. HUISKAMP AND A. VAN OOSTEROM, *IEEE Trans. Biomed. Eng.* **36**, 827 (1989).
10. R. FRANKE, *Math. Comput.* **38**, 181 (1982).
11. C. K. CHUI *et al.* (Eds.), *Topics of Multivariate Approximation, Proceedings, International Workshop, University of Chile, Dec.* 15–19, 1986 (Academic Press, New York, 1987).